# Supplementary material

## A novel intermediate in the $LiAlH_4$-$LiNH_2$ hydrogen storage system

L. H. Jepsen[1], D. B. Ravnsbæk[2], C. Grundlach[3], F. Besenbacher[4], J. Skibsted[5], T. R. Jensen[1*]

[1]*Center for Materials Crystallography, Interdisciplinary Nanoscience Center (iNANO) and Department of Chemistry, Aarhus University, Langelandsgade 140, DK-8000 Aarhus C, Denmark*

[2] *Department of Material Science and Engineering, Massachusetts Institute of Technology, 77 Massachusetts Avenue, Cambridge 02139, MA, USA*

[3] *MAXlab-II Laboratory, Lund University, Ole Romers vag 1, 223 63, S-22100 Lund, Sweden*

[4] *Interdisciplinary Nanoscience Center (iNANO) and Department of Physics and Astronomy, 8000 Aarhus C, Denmark*

[5] *Instrument Centre for Solid-State NMR Spectroscopy, Department of Chemistry, Aarhus University, Denmark.*

*Corresponding author
Torben R. Jensen, Ph.D., Associate Professor
Center for Materials Crystallography
iNANO and Department of Chemistry
Langelandsgade 140
DK-8000 Aarhus C
Aarhus University
Denmark

**Table S1** Observed temperatures for decomposition and formation of listed compounds during *in situ* SR-PXD. All samples are heated from RT with 5 °C/min under dynamic vacuum.

| | **s0** | **s1** | **s2** | **s3** | **s1**(DSC) |
|---|---|---|---|---|---|
| Decomposition of $LiAlH_4$ (°C) | 151 | 162 | 155 | 160 | 174 |
| Decomposition of $Li_3AlH_6$ (°C) | 213 | 206 | 205 | 205 | 209 |
| Reaction between $LiNH_2$ and LiH (°C) | 287 | 296 | 285 | 292 | 298 |
| Formation of $Li_{4-x}Al_x(NH)_{2-2x}N_{2x}$ (°C) | - | 340 | 310 | 315 | |
| Last observation of $Li_2NH$ (°C) | >500 | >500 | 390 | 391 | |
| Formation of $Li_3AlN_2$ (°C) | 410 | 413 | 410 | 408 | |
| Disappearance of Al (°C) | >500 | >500 | 620 | >500 | |

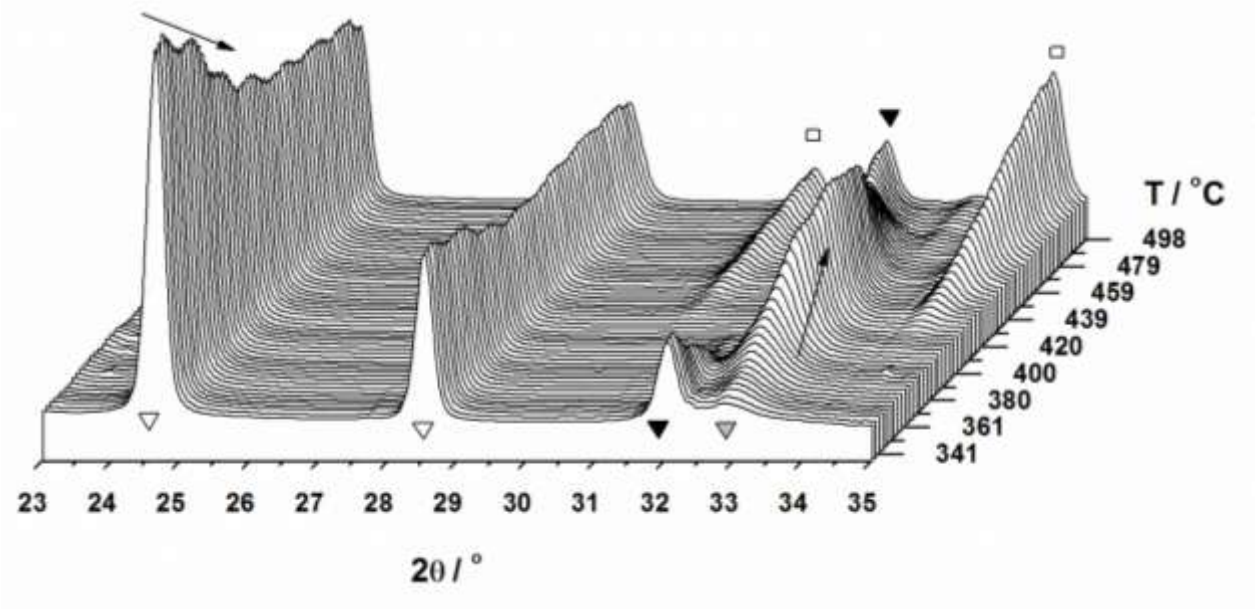


**Figure S1** *In situ* SR-PXD of $LiAlH_4$—$LiNH_2$ (1:2.5, **s3**) heated from RT to 500 °C (5 °C/min, dynamic vacuum, λ = 1.00355 Å). Symbols: ▼ $Li_2NH$; ▽ $Li_{4-x}Al_x(NH)_{2-2x}N_{2x}$; ▽ Al; □ $Li_3AlN_2$. Reflections from Al and $Li_2NH$ decrease and disappear, respectively when $Li_{4-x}Al_x(NH)_{2-2x}N_{2x}$ is formed.

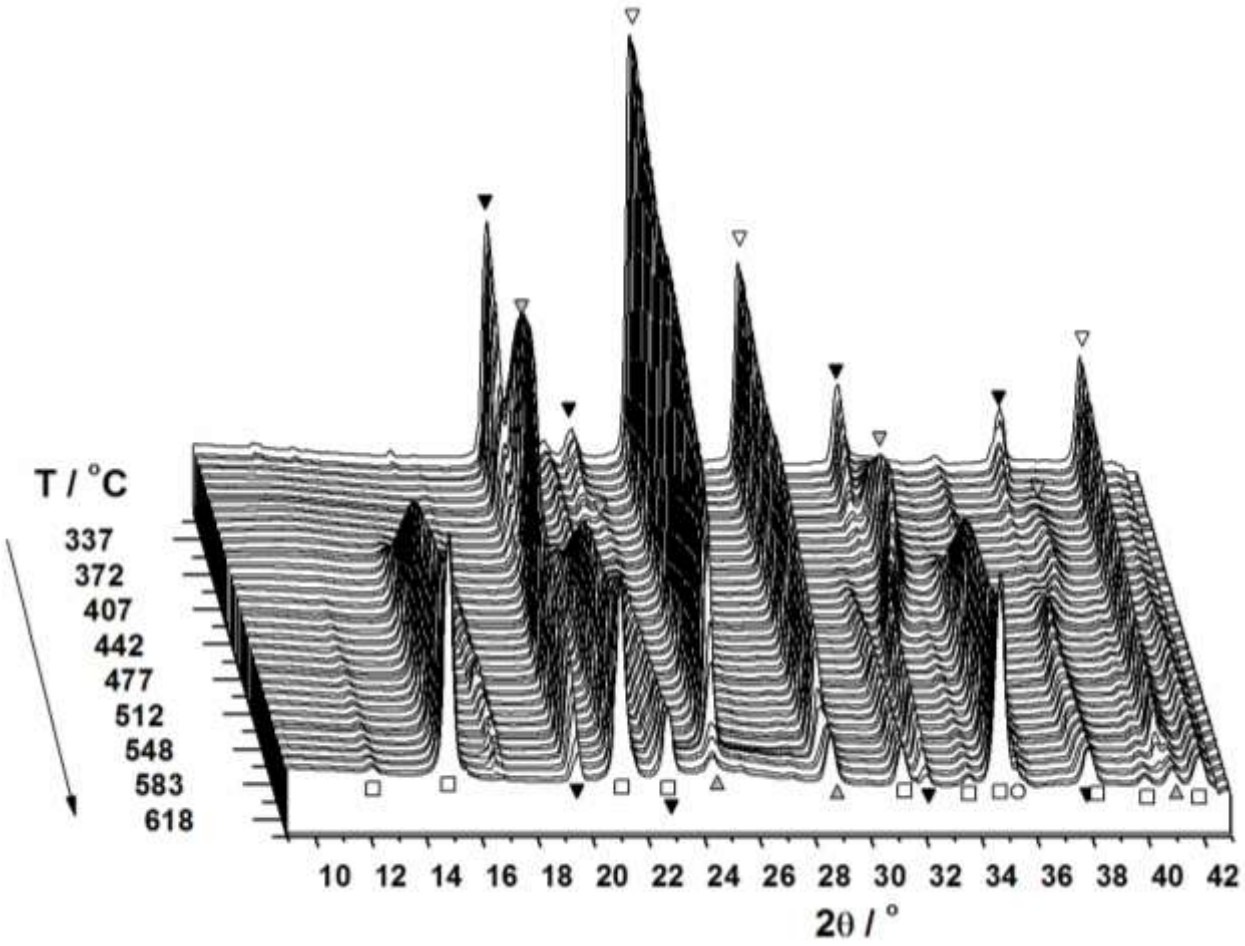


**Figure S2** *In situ* SR-PXD of $LiAlH_4$—$LiNH_2$ (1:2, **s2**) heated from RT to 635 °C (5 °C/min, dynamic vacuum, λ = 1.00989Å). Symbols: ▼ $Li_2NH$; ▽ $Li_{4-x}Al_x(NH)_{2-2x}N_{2x}$; ▽ Al; □ $Li_3AlN_2$; ○ $Li_2O$

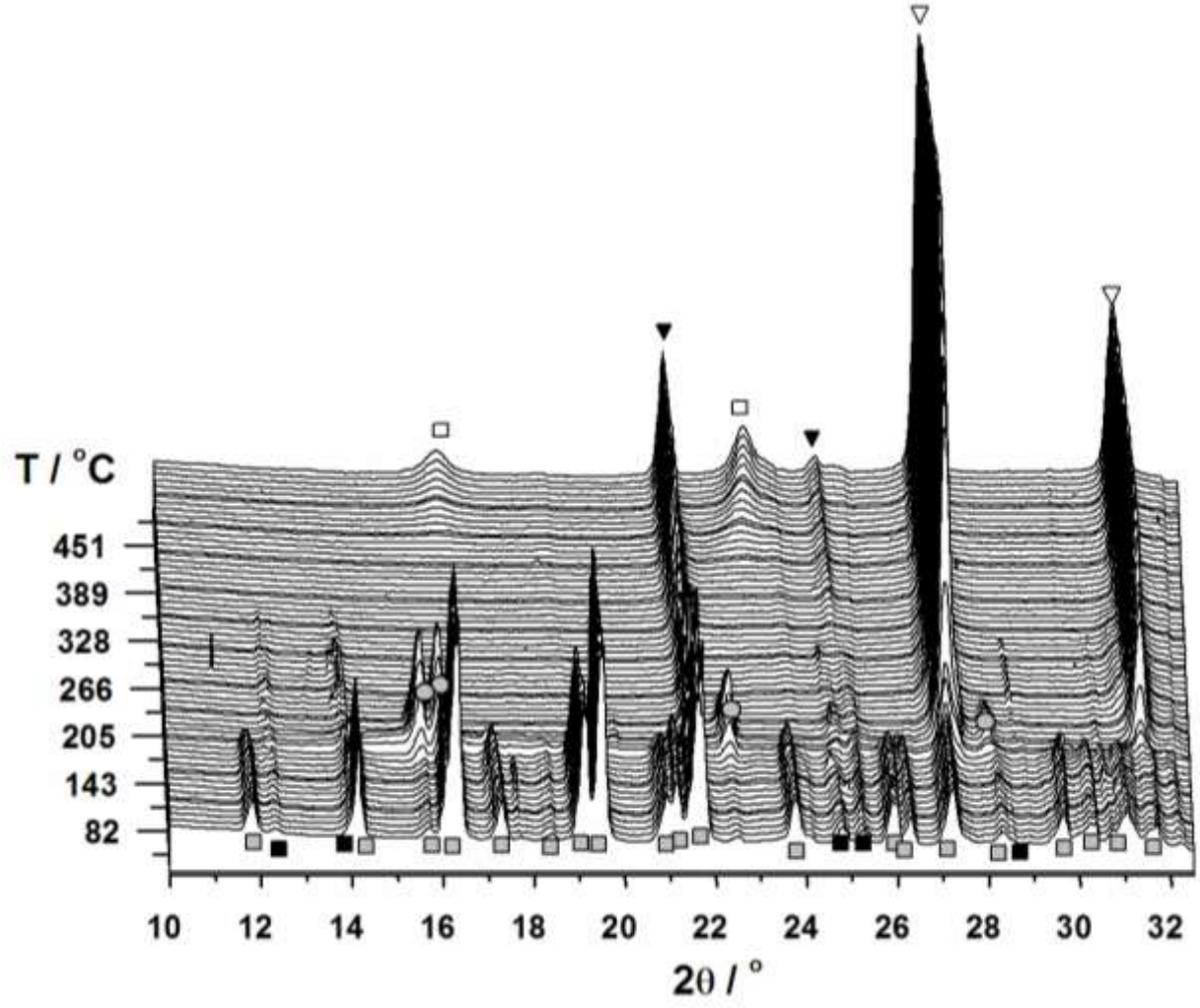


**Figure S3** *In situ* SR-PXD of $LiAlH_4$—$LiNH_2$ (1:1, **s0**) heated from RT to 500 °C (5 °C/min, dynamic vacuum, λ = 1.10205 Å). $Li_2NH$ does not react with Al forming $Li_{4-x}Al_x(NH)_{2-2x}N_{2x}$ in contrast to **s1**, **s2** and **s3**. Symbols: ■ $LiNH_2$; ▩ $LiAlH_4$; ○ $Li_3AlH_6$; ▼ $Li_2NH$; ▽ Al;□ $Li_3AlN_2$.

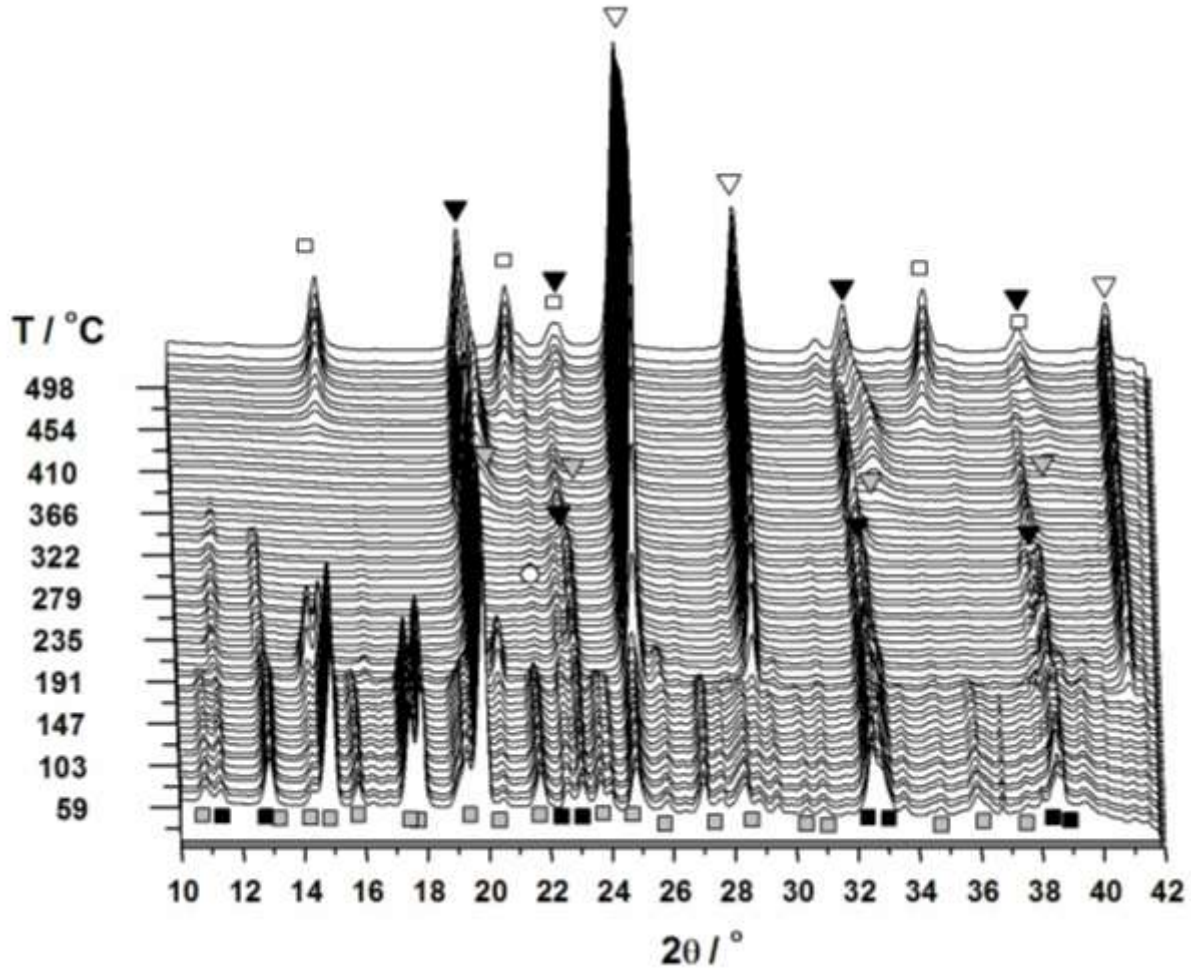


**Figure S4** *In situ* SR-PXD of $LiAlH_4$—$LiNH_2$ (1:1.5, **s1**) heated from RT to 500 °C (5 °C/min, dynamic vacuum, λ = 1.00355 Å). Symbols: ■ $LiNH_2$; ▣ $LiAlH_4$; ○ $Li_3AlH_6$; ▼ $Li_2NH$; ▽ Al □ $Li_3AlN_2$; ▼ $Li_{4-x}Al_x(NH)_{2-2x}N_{2x}$.

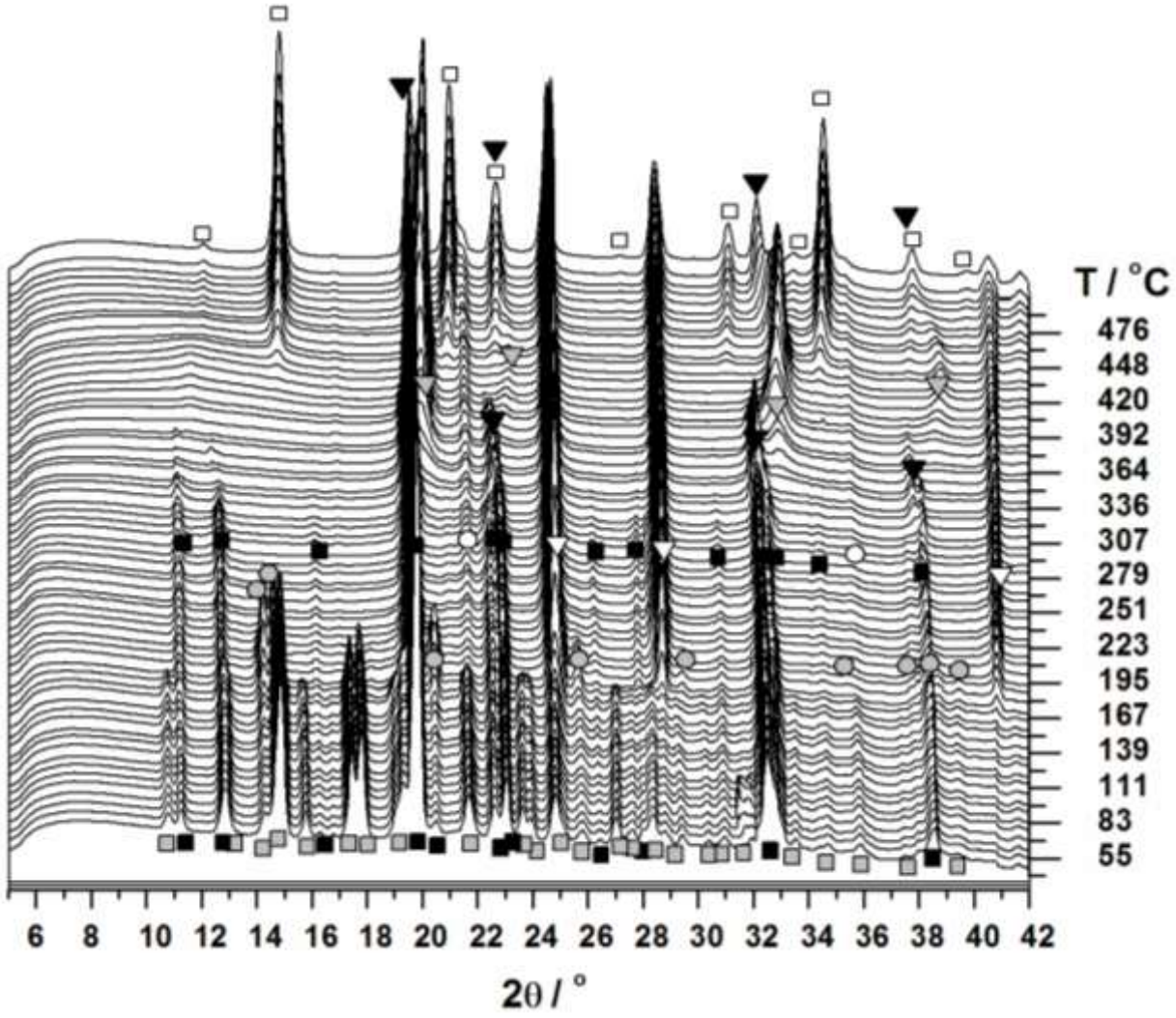


**Figure S5** *In situ* SR-PXD of $LiAlH_4$—$LiNH_2$ (1:2.5, **s3**) heated from RT to 500 °C (5 °C/min, dynamic vacuum, λ = 1.00355 Å). Symbols: ■ $LiNH_2$; ▩ $LiAlH_4$; ○ $Li_3AlH_6$; ▽ $Li_{4-x}Al_x(NH)_{2-2x}N_{2x}$; ▼ $Li_2NH$; ▽ Al; □ $Li_3AlN_2$.

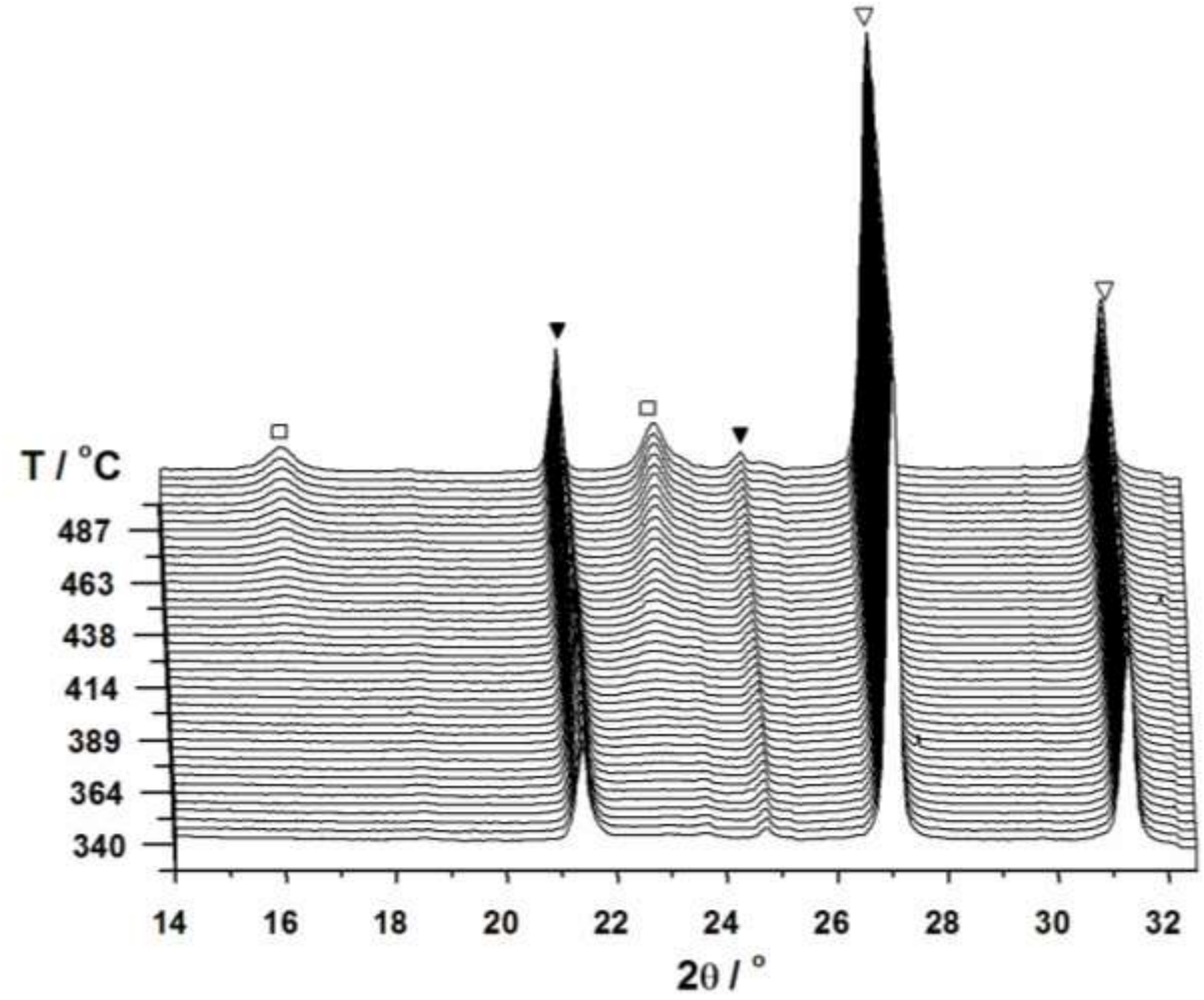


**Figure S6** An expansion of the *in situ* SR-PXD data for $LiAlH_4$—$LiNH_2$ (1:1, **s0**) heated from RT to 500 °C (5 °C/min, dynamic vacuum, λ = 1.10205 Å). In contrast to **s1**, **s2** and **s3**, the formation of $Li_{4-x}Al_x(NH)_{2-2x}N_{2x}$ is not observed. Symbols: ▼ $Li_2NH$; ▽ Al; □ $Li_3AlN_2$;

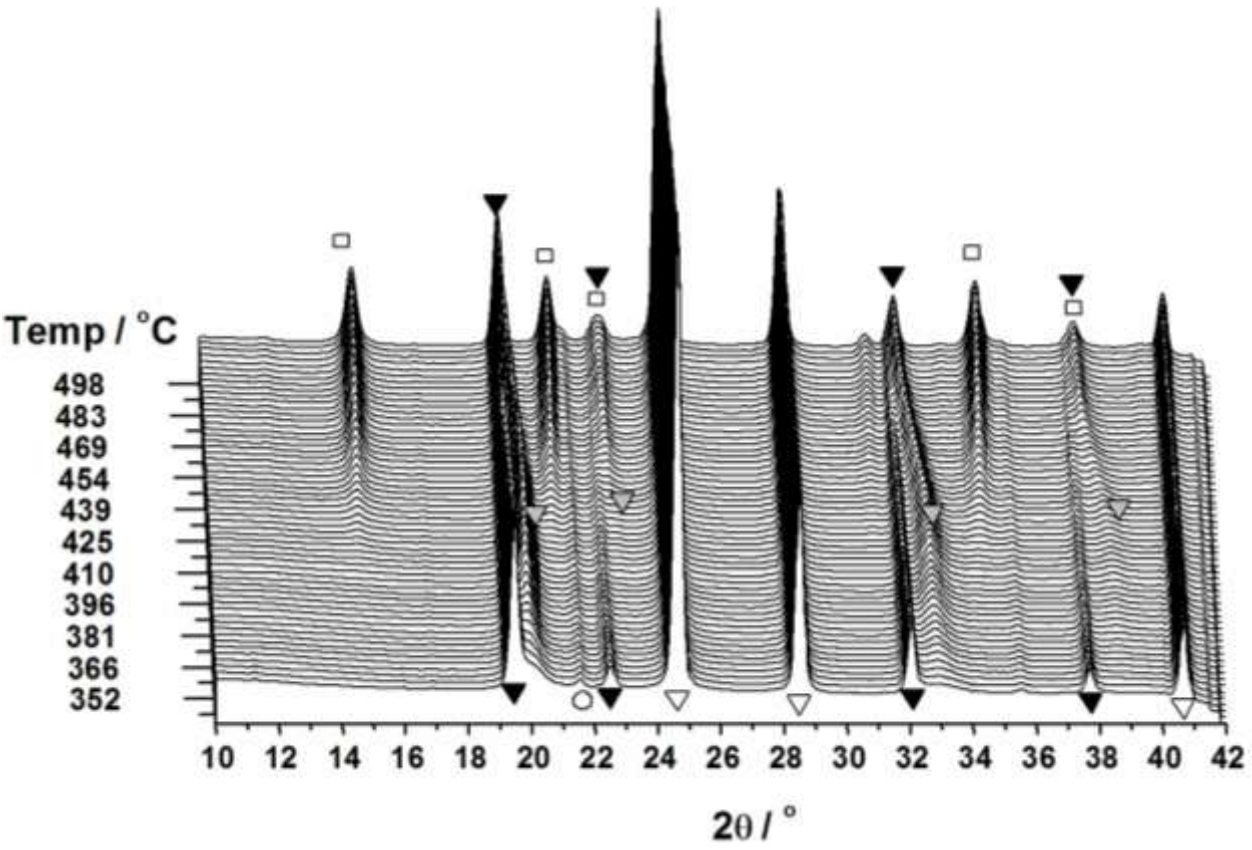


**Figure S7** An expansion of the *in situ* SR-PXD data for $LiAlH_4$—$LiNH_2$ (1:1.5, **s1**) heated from RT to 500 °C (5 °C/min, dynamic vacuum, λ = 1.00355 Å). Only some of $Li_2NH$ is consumed in the reaction with Al forming $Li_{4-x}Al_x(NH)_{2-2x}N_{2x}$ in contrast to **s2** and **s3**, where all $Li_2NH$ reacts with Al. Symbols: ▼ $Li_2NH$; ▽ $Li_{4-x}Al_x(NH)_{2-2x}N_{2x}$; ▽ Al; □ $Li_3AlN_2$; ○ $Li_2O$

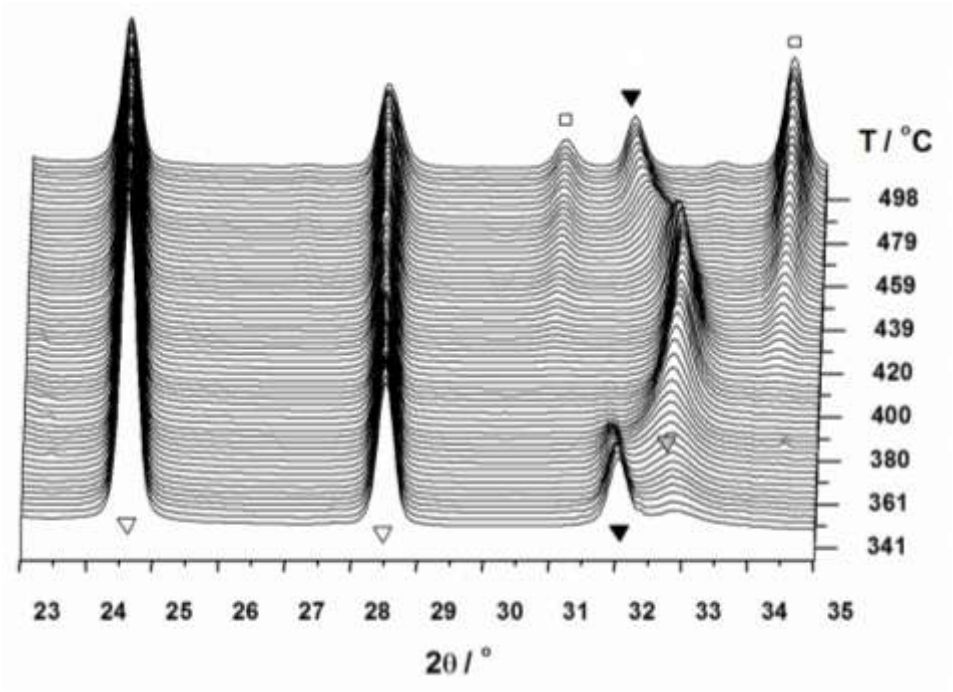


**Figure S8** An expansion of the *in situ* SR-PXD data for $LiAlH_4$—$LiNH_2$ (1:2.5, **s3**) heated from RT to 500 °C (5 °C/min, dynamic vacuum, λ = 1.00355 Å). All $Li_2NH$ is consumed in the reaction with Al forming $Li_{4-x}Al_x(NH)_{2-2x}N_{2x}$ in contrast to s1. Symbols: ▼ $Li_2NH$; ▽ $Li_{4-x}Al_x(NH)_{2-2x}N_{2x}$; ▽ Al; □ $Li_3AlN_2$.

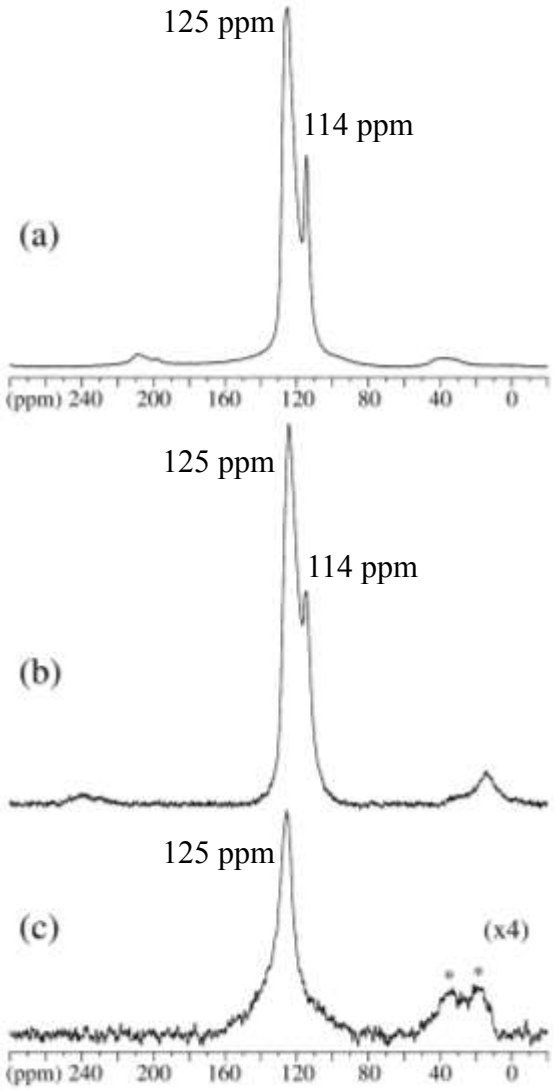


**Figure S9** $^{27}$Al MAS NMR spectra for (a, b) **s2**_465 and (c) **s2**_345, acquired at (a) 14.09 T and (b, c) 9.39 T using spinning speeds of $\nu_R$ = 13.0 kHz and 12.0 kHz, respectively. The spectrum in part (a) is the same spectrum as shown in Figure 4. The $^{27}$Al chemical shift and line broadening for the centerband from $Li_{4-x}Al_x(NH)_{2-2x}N_{2x}$ are almost independent of the magnetic field. The intensity in part (c) is multiplied by a factor of four as compared to the intensity in part (b). The asterisks indicate a static background signal from the 5 mm CP/MAS NMR probe used for the experiments in parts (b, c).

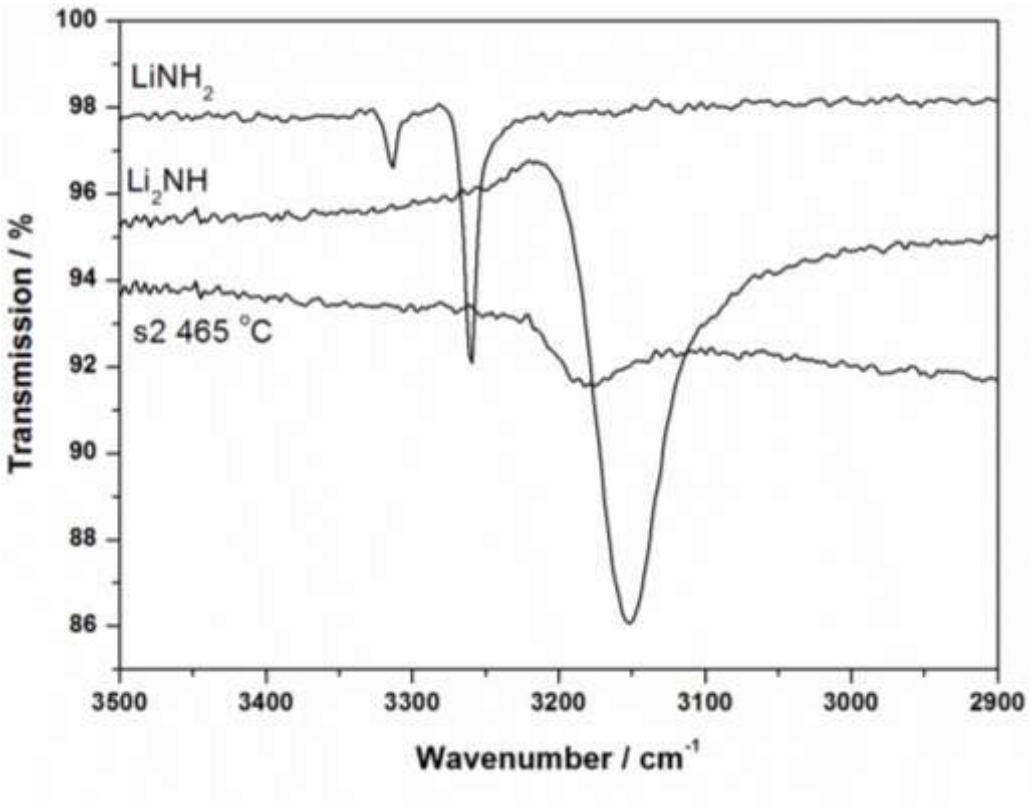


**Figure S10** FTIR data obtained for $LiNH_2$, $Li_2NH$ and s2_465.

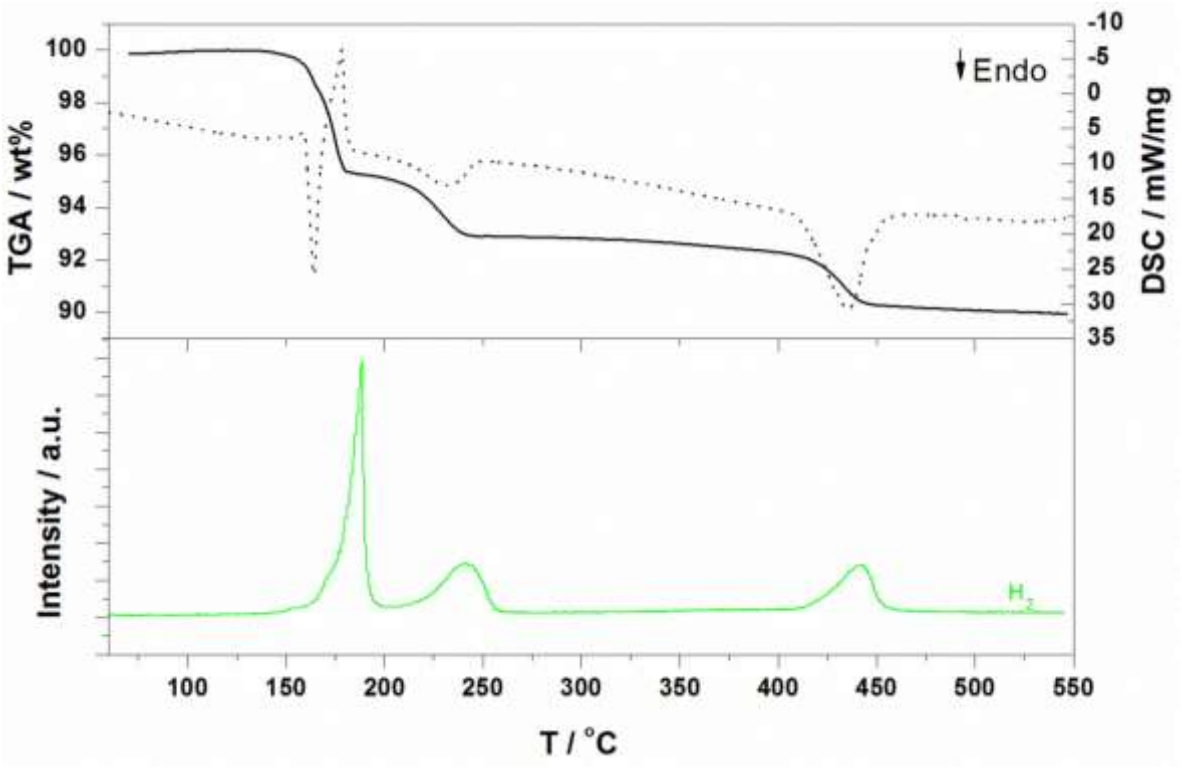


**Figure S11** Upper: TGA (solid) and DSC (dotted) for $LiAlH_4$ heated from RT to 550 °C (5 °C/min). Lower: MS signal detecting $H_2$.

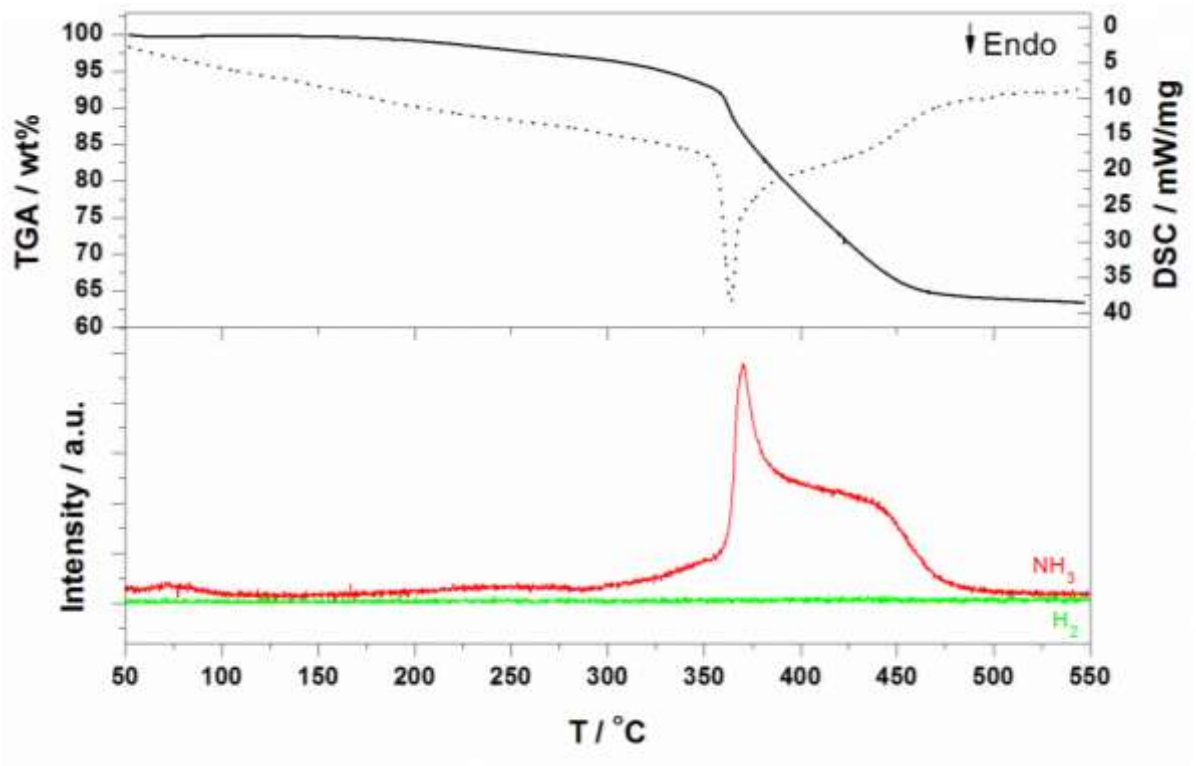


**Figure S12** Upper: TGA (solid) and DSC (dotted) for $LiNH_2$ heated from RT to 550 °C (5 °C/min). Lower: MS signal detecting $NH_3$ (red) and $H_2$ (green).

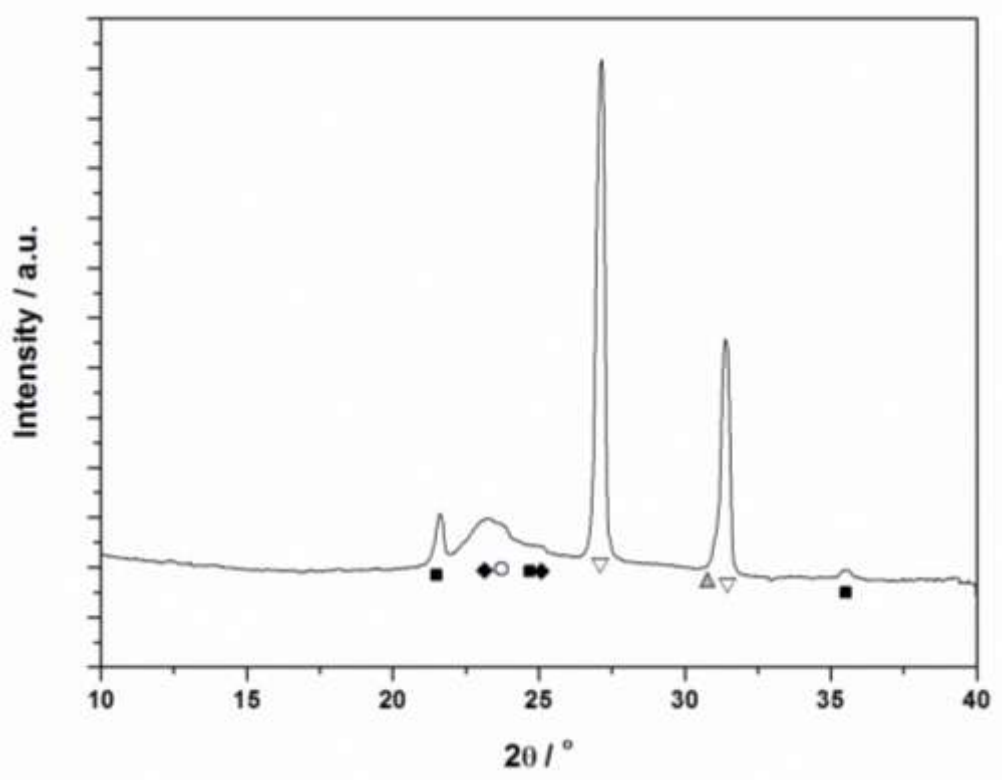


**Figure S13** SR-PXD data for **s0** heated from RT to 500 °C under dynamic vacuum, and subsequently heated to 425 °C $p(H_2)$ = 100 bar and finally cooled to RT, λ = 1.10205 Å. Symbols: ▽ Al; ◆AlN; ○$Li_2O$; △ LiH; ■ $LiNH_2$.